37.0 ADVANCED ENGINEERED COATINGS WITH EXTENDED DIE LIFE FOR TOOLING

Nelson Delfino de Campos Neto (Mines)
Faculty: Stephen Midson, Andras Korenyi-Both and Michael Kaufman (Mines)
Industrial Mentors: Paul Brancaleon (NADCA) and Rob Mayer (Queen City Forging Co.)

This project started in Fall 2018, is a five-year effort, and is supported by the Defense Logistics Agency and CAPES in Brazil. The research performed during this project will serve as the basis for a Ph.D. thesis for Nelson Delfino de Campos Neto.

37.1 Project Overview and Industrial Relevance

Die coatings produced by physical vapor deposition (PVD) started being used in the die casting industry in the 1990s, but at that time the coatings were relatively simple in nature and tended to be used only to minimize soldering of molten aluminum to core pins. Since then, die casters have developed more complex multi-layer coating architectures, and have also started to use the coatings for "lube-free" applications. However, the factors that prevent the die cast aluminum alloys from sticking to the coatings are still not fully understood, precluding optimal coating compositions from being identified. In addition, die coating architectures need to be identified that will allow the coatings to last as long as the dies (~100,000 shots).

The PVD coatings help prevent aluminum die castings from soldering to the die surfaces, allowing the amount of lubricants that are applied to the die to be reduced or even eliminated. Minimizing the use of lubricants will reduce production costs arising from the purchase of the lubricants, the clean-up of effluents, reducing cycle time, and provide an extension in die life, resulting in lower per-part costs. Reduced lubricant also leads to a significant improvement of the quality of die castings, allowing them to be used in higher performance applications. Cost optimization is important for part manufacturers, as die casting is normally the lowest cost approach for producing complex-shaped components from aluminum alloys.

37.2 Previous Work – Literature Review and Background

A prior project was performed at the Colorado School of Mines (Mines) by Wang [37.1], where a variety of PVD coatings were evaluated, finding that AlCrN had the best performance of those tested. The AlCrN coating was applied to a commercial die and a plant trial was conducted at Mercury Castings, where they were able to reduce the use of conventional organic lubricants by ~85% and significantly reduce cycle time. The goal of this current follow-on project is to build on the research performed by Wang, and achieve the complete elimination of conventional lubricants for the die casting process.

The initial phase in the current project involved performing a literature review of several related fields, including brazing, the dissolution of materials by liquid metals, and the wetting and reaction between ceramics and liquid metals. The goal is to identify the types of ceramic coatings that can minimize wetting and soldering during the die casting process. To date, the literature review has primarily focused on understanding wetting behavior. A relevant publication is a recent review paper by Eustathopoulos [37.2], who reviewed the factors controlling the wetting of ceramics by liquid metals, and the concepts reported by Eustathopoulos have been correlated with the results presented by Wang [37.1]. This has enabled the current authors to develop a better understanding of the factors controlling wetting of liquid metals on bare H13 steel and on PVD coatings.

During the first two years of the project, the main focus was on developing an improved aluminum adhesion test, based on the test described in previous reports [37.3-37.5]. The key features of this improved test include i) using bottom pouring to avoid incorporation of the floating oxide layer between the material coupon and the cast aluminum, ii) using induction heating to quickly heat and melt the aluminum alloy, iii) controlling and recording of the temperature of the material coupon during the test, iv) performing melting inside a controlled environment chamber (vacuum + back filling with inert gas), v) pre-heating the casting die and material coupon prior to bottom pouring of the molten aluminum, and vi) rapidly placing the cast aluminum and material coupon into a pre-heated furnace for extended holding times at the desired temperature, to allow for diffusion at the interface between the material coupon and the molten aluminum alloy.

Molten aluminum tests (MAT) were performed on bare H13 and five different AlCrN coatings using the setup described above and the results of these tests have been presented in a previous report [37.5]. Due to different behavior exhibited by the coatings in the MAT, coating characterization techniques were applied to better understand the composition, structure and performance of these coatings.

37.3 Recent Progress

37.3.1 Characterization of five different AlCrN coatings

Five different AlCrN coatings were obtained from two commercial sources. The coatings were produced by cathodic arc evaporation (CAE) and deposited onto polished 25.4 mm by 25.4 mm (1" by 1") substrates of heat treated H13 steel. For simplicity in this paper, the coatings will be referred to as AlCrN-1 through AlCrN-5, and the designations for the five coatings are summarized in **Table 37.1**. The first coating, AlCrN-1, was supplied in the as-deposited condition. The second coating, AlCrN-2, received a post-deposition polishing treatment (PDPT). The third coating, AlCrN-3, contained a relatively high carbon content and was supplied in the as deposited condition. The fourth coating, AlCrN-4, was supplied in the as-deposited condition by a second supplier. Finally, the last coating, AlCrN-5, was deposited on H13 coupons that had been nitrided using ion implantation.

A variety of techniques were utilized to characterize the coatings, including calo testing, optical profilometry, scratch testing, VDI 3198 Rockwell C indentation, pin-on-disk, X-ray photoelectron spectroscopy (XPS), scanning electron microscopy (SEM) with energy dispersive spectroscopy (EDS), focused ion beam (FIB), and transmission electron microscopy (TEM).

37.3.2 Results from the characterization techniques applied to AlCrN coatings

The thickness of the five AlCrN coatings were estimated using three techniques, calo testing (ball cratering), SEM analysis on polished cross sections, and via observations in the TEM. The results are summarized in **Table 37.2**. All three methods found similar thickness values for each coating. The coatings from supplier 2, AlCrN-4 and AlCrN-5, were much thicker than the other coatings. It is not clear exactly how the coating thicknesses will affect performance, although Bell et al. [37.6] noted that PVD coatings are normally not thicker than 5-6 μm due to the brittle nature of thick coatings.

The compositions of the five coatings were estimated using XPS measurements, and the compositions reported in **Table 37.3** are the averages between XPS measurements after 20 and 40 minutes of argon ion cleaning. The AlCrN-1 and AlCrN-2 coatings have similar compositions and are slightly under-stoichiometric in N concentration. The AlCrN-3 coating, however, has a significantly different composition, with relatively large concentrations of carbon and titanium, even though the coating is marketed commercially as AlCrN, although the presence of carbon is mentioned in the marketing materials. The AlCrN-4 and AlCrN-5 coating has a stoichiometric (Al,Cr)-N composition relative to N and a lower Al/Cr ratio (~1.4) than AlCrN-1 and AlCrN2, where the Al/Cr ratio is around 3.5.

Surface roughness has been shown to have a significant effect on soldering and coating performance in aluminum die casting [37.7-37.9]. The roughness measurements for the coatings examined in this study performed using optical profilometry are shown in **Table 37.4**. The coatings are smooth with low Ra values in the nanometer scale and without much difference between coatings, but the coatings from supplier 2 (AlCrN-4 and AlCrN-5) presented a tendency to higher roughness values that may be the result of these coating being much thicker.

Cohesion within the coatings and adhesion to the substrates were estimated using the scratch test and VDI 3198 measurements and the results are shown in **Table 37.5**. Cohesion is a measure of the quality of the coatings, while adhesion measures how well the coatings are adhered to the H13 steel substrates. The cohesive critical loads (Lc_1) were in the range from 6-9 N for all coatings, suggesting they are of similar quality. All three coatings from supplier 1 (AlCrN-1, AlCrN-2 and AlCrN-3) exhibited similar adhesive critical loads (Lc_2) of around 15 N, higher in comparison to those for AlCrN-4 (11.3 N) but smaller than AlCrN-5 (~23 N). VDI 3198 tests were used to complement the scratch tests, and the optical analysis of the indentation marks indicated excellent adhesion to the substrate, all five being indexed as HF1 [37.10].

Pin-on-disk measurements have been used to understand the wear behavior of coatings used in aluminum die casting [37.7]. The results of the pin-on-disk measurements performed in this study are shown in **Table 37.6**, showing

considerable differences between the coatings. The AlCrN-1 and AlCrN-2 coatings exhibited a high and almost constant coefficient of friction (COF) of about 0.80 and a large amount of wear in these two coatings occurred as a consequence of this COF value. The AlCrN-3 coating exhibited a non-constant friction behavior during the test, where the measured data suggest first an accommodation period with a higher COF about 1.02 (referred to here as stage 1) followed by a substantial drop in the COF to around 0.30 (referred to here as stage 2). As a result of this lower COF, the wear for the AlCrN-3 coating was much smaller in comparison to the wear for the other four coatings. The AlCrN-4 (COF of 0.56) and AlCrN-5 (COF of 0.51) coatings exhibited relatively constant COFs that were smaller in comparison with AlCrN-1 and AlCrN-2, but higher than the stage 2 COF for AlCrN-3.

SEM backscattered electron (BSE) images and EDS maps of polished cross sections through the AlCrN-1 and AlCrN-2 coatings (**Figure 37.1**) indicate that both bond coatings have a Ti/TiN adhesion layer of considerable thickness (~25% of total coating thickness). **Figure 37.1c** also shows a Ti/TiN adhesion layer for the AlCrN-3 coating but, unlike the other two coatings, for the AlCrN-3 coating titanium also appears to be part of the coating structure. In contrast, the AlCrN-4 (**Figure 37.1d**) and AlCrN-5 (**Figure 37.1e**) coatings do not use a Ti/TiN bond layer. Rather, these coatings use a thin Cr/CrN adhesion layer to the H13 prior to the thick growth of the AlCrN coating. However, the differences in the compositions and thicknesses of the adhesion layers do not appear to significantly affect the performance of the coatings, as the scratch test and VDI 3198 results suggest that all the coatings are dense and well bonded to the H13 substrate.

To better understand the coating microstructures, higher magnification analysis was carried out in the transmission electron microscope (TEM) conducted on FIB liftouts. Only the microstructures of two of the coatings are shown here. The AlCrN-1, AlCrN2, AlCrN-4 and AlCrN-5 coatings were all monolithic in nature, consisting of the adhesion layer and the AlCrN top coatings. **Figure 37.2a** shows the structure of the AlCrN-2 coating, which from left-to-right shows the H13 steel substrate, the adhesion layer, and the AlCrN single layer coating. However, the microstructure of the AlCrN-3 coating was significantly different, as it consisted of a complex, multi-nanolayered structure. **Figure 37.2b** shows a HAADF image from the AlCrN-3 coating showing it consists of 80 nm regions that contain alternating ~2 nm thick nano-layers separated by 35 nm regions that are not modulated. While the EDS line scan in **Figure 37.2c** indicates that the darker nanolayers are slightly enriched in Al while the brighter layers are enriched in Cr, the differences appear to be small, possibly due to measurement problems arising from beam spreading and spatial resolution issues resulting from the small dimensions of the nanolayers. The thicker (35 nm) brighter layer is slightly higher in Ti than in the alternating nanolayers, along with a corresponding decrease in Cr.

37.4 Plans for Next Reporting Period

- Continue to evaluate the published literature to characterize wetting, PVD coatings, chemical interactions between liquid metals and ceramics, and brazing.
- Continue the experimental work using the new test apparatus and start a first round of industry trials in selected coatings.
- Characterization of the PVD coated samples using a range of techniques: electron microscopy, tribology, and surface analysis.
- Characterization of the soldered surfaces to understand solder and adhesion, interdiffusion, phase formation, and defects.

37.5 Acknowledgements

- This program is sponsored by the Defense Logistics Agency – Troop Support, Philadelphia, PA and the Defense Logistics Agency Information Operations, J68, Research & Development, Ft. Belvoir, VA.
- N.D. Campos Neto is thankful to CAPES Brazil for a scholarship from the program DOC-PLENO - Full Doctorate Abroad - Call No. 48/2017 - Selection 2018 process number 88881.175453/2018-01.

37.6 References

[37.1] B. Wang, An Investigation of the Adhesion Behavior of Aluminum on Various PVD Coatings Applied to H13 Tool Steel to Minimize or Eliminate Lubrication During High Pressure Die Casting, PhD thesis, CSM, 2016.

[37.2] N. Eustathopoulos, Wetting by Liquid Metals—Application in Materials Processing: The Contribution of the Grenoble Group, Metals 5, 2015, 350-370.

[37.3] N. D. Campos Neto, A. Korenyi-Both, S. Midson, M. J. Kaufman. Advanced Engineered Coatings with Extended Die Life for Tooling. CANFSA Biannual Report, Project 37, March 25, 2019.

[37.4] N. D. Campos Neto, A. Korenyi-Both, S. Midson, M. J. Kaufman. Advanced Engineered Coatings with Extended Die Life for Tooling. CANFSA Biannual Report, Project 37, October 2, 2019.

[37.5] N. D. Campos Neto, A. Korenyi-Both, S. Midson, M. J. Kaufman. Advanced Engineered Coatings with Extended Die Life for Tooling. CANFSA Biannual Report, Project 37, April 7, 2020.

[37.6] D. Bell, V. Khominich, S, Midson, C. Mulligan, High Quality PVD Coatings for Corrosion Protection Applications, Materials Performance, 58, No. 6, 2019.

[37.7] J.M. Paiva, G. Fox-Rabinovich, E.L. Junior, P. Stolf, Y.S. Ahmed, M.M Martins, C. Bork, S. Veldhuis, Tribological and wear performance of nanocomposite PVD hard coatings deposited on aluminum die casting tool, Materials, 11, 358, 2018.

[37.8] S. Gulizia, M.Z. Jahedi, E.D. Doyle, Performance evaluation of PVD coatings for high pressure die casting, Surface and Coatings Technology, 140, 200-205, 2001.

[37.9] P. Terek, L. Kovačević, A. Miletić, P. Panjan, S. Baloš, B. Škorić, D. Kakaš, Effects of die core treatments and surface finishes on the sticking and galling tendency of Al–Si alloy casting during ejection, Wear, 356-357, 122-134, 2016.

[37.10] N. Vidakis, A. Antoniadis, N. Bilalis, The VDI 3198 indentation test evaluation of a reliable qualitative control for layered compounds, Journal of Materials Processing Technology, v. 143-144, 481-485, 2003.

37.7 Figures and Tables

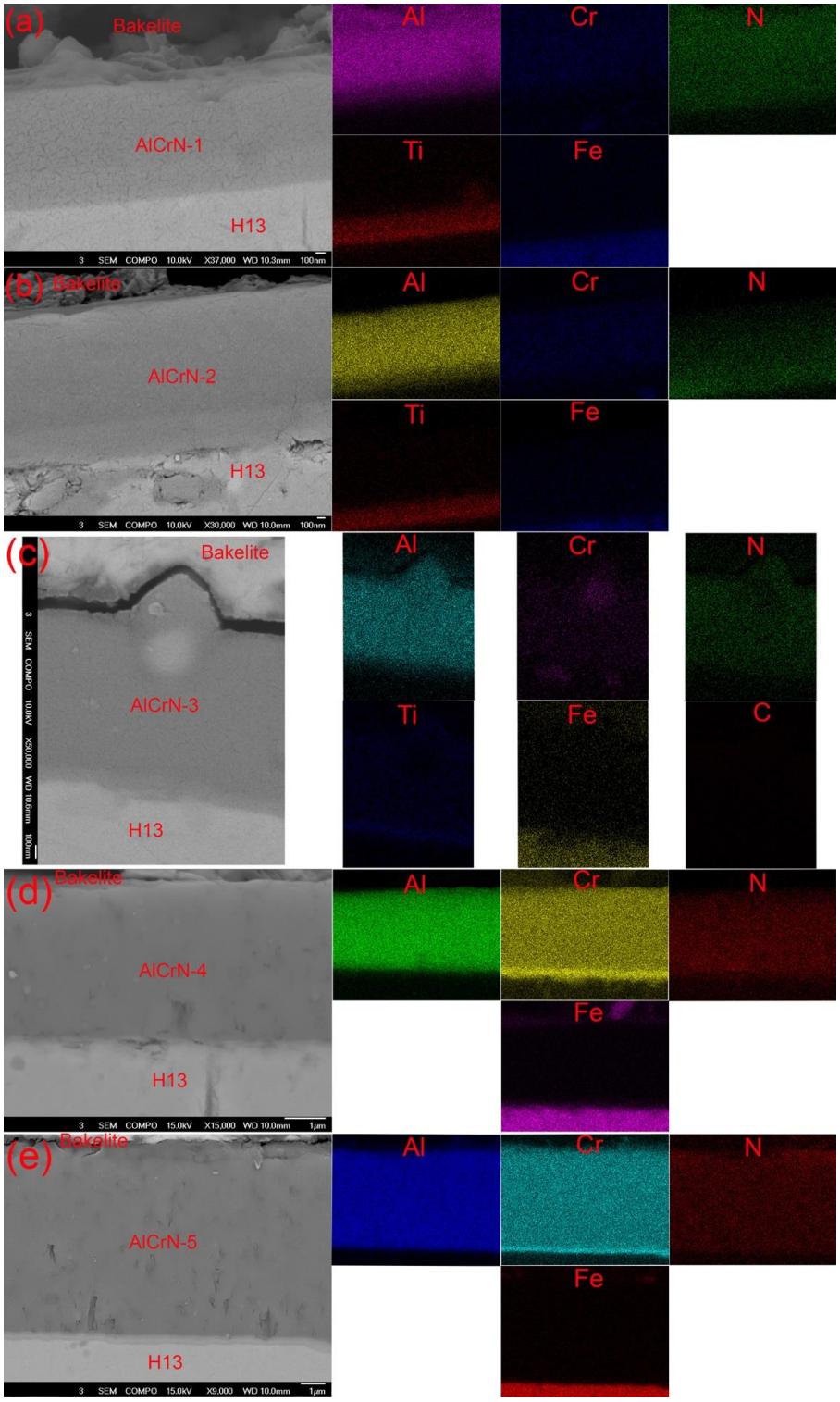

Figure 37.1: SEM BSE images and EDS maps of coating cross-sections: (a) AlCrN-1, (b) AlCrN-2, (c) AlCrN-3, (d) AlCrN-4, and (e) AlCrN-5.

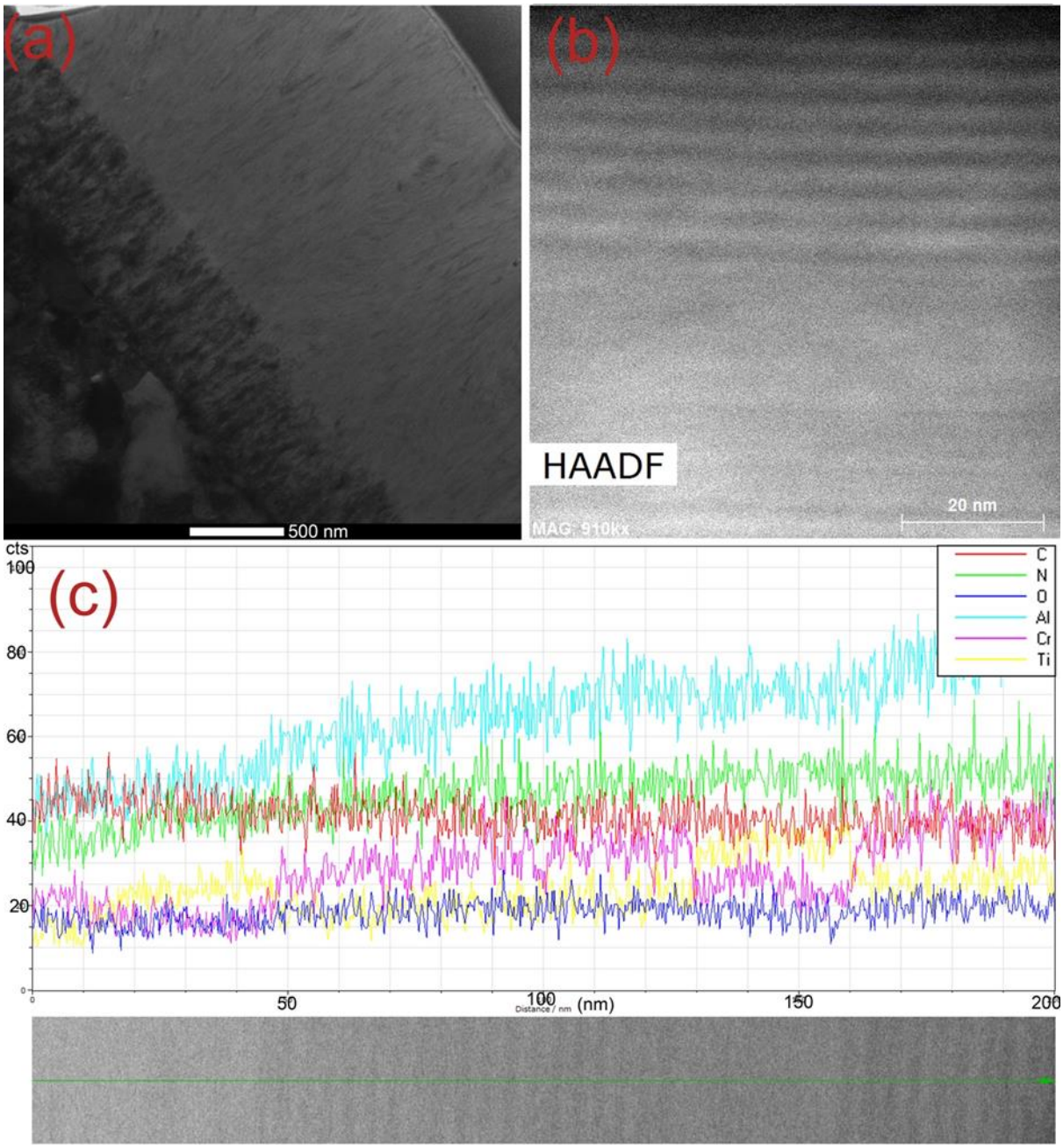

Figure 37.2: TEM/STEM analysis of coating microstructures. (a) TEM BF image of AlCrN-2 coating single layer, (b) STEM HAADF image of the AlCrN-3 coating showing multilayer nanostructure of coating, and (c) EDS linescan of AlCrN-3 coating showing the elemental distribution within the nanolayers of the coating.

Table 37.1: Designation of coatings examined in this study.

Coating Number	Supplier	Coating Description
AlCrN-1	1	AlCrN
AlCrN-2	1	AlCrN-PDPT
AlCrN-3	1	AlCrN - high carbon content
AlCrN-4	2	AlCrN
AlCrN-5	2	AlCrN + ion implanted nitrided layer

Table 37.2: Measured coating thicknesses.

Coating	Thickness (µm)		
	SEM	Calo	TEM
AlCrN-1	1.2 ± 0.1	1.1 ± 0.1	-
AlCrN-2	2.1 ± 0.2	2.0 ± 0.1	2.4 ± 0.1
AlCrN-3	1.3 ± 0.1	1.4 ± 0.1	-
AlCrN-4	6.6 ± 0.4	8.5 ± 0.3	-
AlCrN-5	8.4 ± 0.2	8.9 ± 0.3	-

Table 37.3: Coating composition from XPS measurements.

Coating	Composition (at. %)				
	Al	Cr	N	C	Ti
AlCrN-1	42.5 ± 0.8	11.1 ± 0.4	46.5 ± 0.4	-	-
AlCrN-2	40.4 ± 2.0	12.2 ± 0.8	47.5 ± 1.3	-	-
AlCrN-3	5.7 ± 2.0	1.6 ± 0.4	3.7 ± 0.1	80.2 ± 0.7	9.0 ± 3.0
AlCrN-4	33.9 ± 1.0	19.0 ± 0.7	47.0 ± 0.3	-	-
AlCrN-5	29.3 ± 3.6	21.0 ± 0.5	49.8 ± 4.1	-	-

Table 37.4: Coating roughness from optical profilometry measurements.

Coating	Ra (nm)	Rq (nm)	Rz (µm)	Rt (µm)
AlCrN-1	66 ± 6	87 ± 7	1.90 ± 0.35	4.99 ± 2.09
AlCrN-2	80 ± 5	103 ± 6	1.69 ± 0.29	3.66 ± 0.60
AlCrN-3	92 ± 22	119 ± 30	1.78 ± 0.20	3.68 ± 0.72
AlCrN-4	113 ± 17	144 ± 23	2.46 ± 0.27	4.95 ± 0.95
AlCrN-5	100 ± 13	127 ± 14	1.95 ± 0.03	3.38 ± 0.55

Table 37.5: Coating mechanical properties given by the critical loads Lc_1 and Lc_2.

Coating	Lc_1	Lc_2
AlCrN-1	7.2 ± 0.2	14.6 ± 1.0
AlCrN-2	7.3 ± 0.3	14.9 ± 1.3
AlCrN-3	6.5 ± 0.3	14.7 ± 0.8
AlCrN-4	6.0 ± 0.5	11.3 ± 0.9
AlCrN-5	8.7 ± 2.0	23.0 ± 6.1

Table 37.6: Wear resistance tested by pin-on-disk measurements showing the COF of the five coatings.

Coating	Coefficient of Friction
AlCrN-1	0.80 ± 0.07
AlCrN-2	0.76 ± 0.07
AlCrN-3	Stage 1 - 1.02 ± 0.23 Stage 2 - 0.30 ± 0.14
AlCrN-4	0.56 ± 0.08
AlCrN-5	0.51 ± 0.10